JBC Papers in Press. Published on March 29, 2019 as Manuscript RA119.007492
The latest version is at http://www.jbc.org/cgi/doi/10.1074/jbc.RA119.007492

Proteomic discovery of substrates of the cardiovascular protease ADAMTS7

Alain Colige[1], Christine Monseur[1], James T.B. Crawley[2], Salvatore Santamaria[2], Rens de Groot[2*]

From the [1]Laboratory of Connective Tissue Biology, GIGA, University of Liège, Sart-Tilman 4000 Liège, Belgium; [2] Centre for Haematology, Imperial College London, W12 0NN London, UK

Running title: *ADAMTS7 substrate specificity*

*****To whom correspondence should be addressed: Rens de Groot, Imperial College London, Centre for Haematology, 5th Floor Commonwealth Building, Hammersmith Hospital Campus, Du Cane Road, W12 0NN London, United Kingdom; R.deGroot@imperial.ac.uk; Tel. ++44 (0)20 83 83 22 98

Keywords: ADAMTS7, LTBP4, tissue inhibitor of metalloproteinase (TIMP), TIMP-4, substrate specificity, proteolysis, proteolytic enzyme, ADAMTS, cleavage sites.

ABSTRACT

The protease ADAMTS7 functions in the extracellular matrix (ECM) of the cardiovascular system. However, its physiological substrate specificity and mechanism of regulation remain to be explored. To address this, we conducted an unbiased substrate analysis using terminal amine isotopic labeling of substrates (TAILS). The analysis identified candidate substrates of ADAMTS7 in the human fibroblast secretome, including proteins with a wide range of functions, such as collagenous and non-collagenous ECM proteins, growth factors, proteases, and cell-surface receptors. It also suggested that autolysis occurs at Glu729–Val730 and Glu732-Ala733 in the ADAMTS7 spacer domain, which was corroborated by N-terminal sequencing and western blotting. Importantly, TAILS also identified proteolysis of the latent TGF-β–binding proteins 3 and 4 (LTBP3/4) at a Glu–Val and Glu–Ala site, respectively. Using purified enzyme and substrate, we confirmed ADAMTS7-catalyzed proteolysis of recombinant LTBP4. Moreover, we identified multiple additional scissile bonds in an N-terminal linker region of LTBP4 that connects fibulin-5/tropoelastin and fibrillin-1–binding regions, which have an important role in elastogenesis. ADAMTS7-mediated cleavage of LTBP4 was efficiently inhibited by the metalloprotease inhibitor TIMP-4, but not by TIMP-1 and less efficiently by TIMP-2 and TIMP-3. As TIMP-4 expression is prevalent in cardiovascular tissues, we propose that TIMP-4 represents the primary endogenous ADAMTS7 inhibitor. In summary, our findings reveal LTBP4 as an ADAMTS7 substrate, whose cleavage may potentially impact elastogenesis in the cardiovascular system. We also identify TIMP-4 as a likely physiological ADAMTS7 inhibitor.

ADAMTS7 is an extracellular metalloprotease and one of 19 human ADAMTS family members (1). It is a large protein (>250 kDa), consisting of 15 domains (Fig 1A). A Prodomain, located N-terminal to the metalloprotease (MP) domain, is predicted to maintain latency until it is removed by proprotein convertases. The MP domain is typical for that of metzincin metalloproteases, which contain an active site of three histidines and a catalytic glutamic acid (2). The domains C-terminal of the MP domain most likely provide exosites that enhance substrate binding and specificity, based on studies of other ADAMTS family members (3-5).

The physiological function of ADAMTS7 is not known, but recent evidence shows that it functions in the extracellular matrix (ECM) of cardiovascular tissues (6-10). Analysis of normal expression of ADAMTS7 in healthy adult tissues shows it is predominantly expressed in the heart and in the tunica media of the lung vasculature, but also at lower levels in other tissues, including tendon (1,7,11). In the arterial wall, ADAMTS7 is upregulated in response to injury/inflammation (7,8). In this setting, it influences vascular smooth muscle cell (VSMC) migration, possibly by affecting the composition/integrity of the extracellular matrix (ECM) and/or by influencing the availability of growth factors. Genome Wide Association Studies (GWAS) have established

ADAMTS7 as a susceptibility locus for coronary artery disease (CAD)(6,12) and atherosclerosis is reduced in *Adamts7*$^{-/-}$ mice (7). ADAMTS7 has been detected around VSMCs (and macrophages) in human atherosclerotic plaques and elevated ADAMTS7 staining in the vessel wall has been associated with a high-risk plaque phenotype (7,9,13).

Physiologically, protease activity is often regulated by endogenous inhibitors. Several metalloprotease families are regulated by the Tissue Inhibitor of Metalloprotease (TIMP) family of inhibitors, which in humans consist of four members (TIMP1-4)(14). Whereas all four TIMPs inhibit many members of the Matrix Metalloprotease (MMP) family, ADAMTS1,2,4 and 5 are only inhibited by TIMP-3 (14). For ADAMTS7, like most other ADAMTS family members, inhibition by TIMPs has not been investigated.

The substrate specificity of ADAMTS7 is poorly characterised. Only two proteins, cartilage oligomeric matrix protein (COMP) and thrombospondin 1 (TSP1) have previously been reported as substrates, without identification of cleavage sites (10,15). Moreover, a comprehensive analysis of the substrate repertoire and cleavage sites of ADAMTS7 has not been conducted. Knowledge of the cleavage sites is important for the understanding of the functional consequences of proteolysis. It can also guide the design of (therapeutic) inhibitors that derive selectivity and potency from mimicking substrate residues flanking the cleavage site. It is essential to identify the physiological targets of ADAMTS7 to enable a causal link to be established between ADAMTS7 function and CAD/atherosclerosis. To this end, we used Terminal Amine Isotopic Labelling of Substrates (TAILS), which is a method that employs the labelling of neo-N termini generated by proteolysis to identify and quantify cleavage products by mass spectrometry-based proteomics (LC-MS/MS)(16).

Results

TAILS analysis

To study the substrate specificity of ADAMTS7, we employed TAILS. For this, recombinant ADAMTS7 and truncated variants thereof were generated and expressed (Fig 1). The truncated variant ADAMTS7-Mu, which consists of the first ten N-terminal domains, was expressed at the highest levels and was therefore used in this study. As a control for proteolysis, we generated an inactive variant, ADAMTS7-Mu(E389Q) in which the glutamic acid in the active site of the MP domain (Glu389) is mutated to glutamine, a mutation commonly made to render metzincin proteases inactive (2). As a source of endogenously expressed extracellular matrix substrates we used human fibroblasts. These were co-cultured with HEK cells stably transfected with either ADAMTS7-Mu or the inactive ADAMTS7-Mu(E389Q) for 48 hours and the conditioned medium was used for iTRAQ labelling of new N-termini that are generated by proteolysis. Analysis of the LC-MS/MS results identified forty-five extracellular and transmembrane proteins that exhibited evidence of increased proteolysis in the presence of ADAMTS7-Mu versus ADAMTS7-Mu(E389Q) (Table S1). This list of candidate substrates includes proteins with a wide range of functions, such as collagenous and non-collagenous ECM proteins, growth factors, proteases and cell surface receptors. Interestingly, ADAMTS7 itself was among the candidate substrates (Table S2), suggesting autolytic reactions. Although enrichment of neo-N termini in the presence of active ADAMTS7 suggests that the new N-terminus results from proteolysis by ADAMTS7, targets require verification, as indirect effects such as the upregulation or activation of other proteases provide alternative explanations.

Autolysis at Glu-Ala/Val bonds

To verify that ADAMTS7 cleaves itself, as suggested by TAILS, we reassessed the Western blot of one of the truncated ADAMTS7 variants, ADAMTS7-T4, which also showed potential evidence of autolysis (Fig 1C). This variant lacks the highly glycosylated mucin-like domain, which greatly reduces the molecular weight (MW) of any C-terminal fragment arising from autolysis that can be detected with an anti-myc tag antibody (Ab). On Western blot of ADAMTS7-T4, detecting with an anti-myc Ab, a band corresponding to the zymogen (>110 kDa), which has the Prodomain still attached, was resolved from the mature, active form (<110 kDa), which has the Prodomain removed (Fig 2A). An unexpected, low MW band of 45 kDa, we hypothesised, could be a product of

autolysis. This band would correspond to a C-terminal cleavage product generated by autolysis in the Spacer domain. To confirm the identity of these bands, ADAMTS7-T4 was incubated with furin, a subtilisin-like proprotein convertase which is responsible for Prodomain removal in the ADAMTS family (1,17). The >110 kDa band, corresponding to the ADAMTS7 zymogen, disappeared after incubation with furin (Fig 2A). In addition, the mature form (<110 kDa) and the suspected autolytic cleavage product (45 kDa), were both absent when the furin inhibitor Decanoyl-RVKR-CMK was added during expression. Moreover, a mutant in which the furin cleavage sites were mutated, FCSM (R68A/R70A/R232A/R236A), also showed the >110 kDa band (zymogen) only, which confirms that the Prodomain maintains latency and thus prevents generation of the 45 kDa autolytic cleavage product. The inactive ADAMTS7-T4(E389Q) variant also lacked the 45 kDa band, further confirming its generation is dependent on ADAMTS7 activity.

To identify the scissile bond that is targeted in this autolytic reaction, we isolated the 45 kDa cleavage product for N-terminal sequencing. The N-terminal sequence was identified as "AANFL", which matches an abundant autolytic product identified by TAILS (AANFLALR) (Table S2). This new N-terminus is generated by autolysis at the Glu732-Ala733 bond in the Spacer domain. Interestingly, the adjacent and similar Glu729-Val730 bond is also a major target, as demonstrated by abundant VAEAANFLALR peptide identified by TAILS.

As both the Glu729-Val730 and the Glu732-Ala733 bond contain a glutamic acid residue in the P1 position, we mutated these to alanine to investigate the preference of ADAMTS7 for a glutamic acid residue in P1. The mutant ADAMTS7-T4 (E729A/E732A) showed markedly reduced autolysis (Fig. 2B), showing that glutamic acid residues are better accommodated in the S1 pocket of ADAMTS7, compared to alanine. However, a faint 45 kDa band was still visible, showing that Ala in P1 permits proteolysis, but at a reduced rate.

To visualise the location of these autolytic cleavage sites in the structure of ADAMTS7, we modelled the structure of the N-terminal domains of ADAMTS7 (MP-Spacer) using the structure of ADAMTS13 as a template. This revealed that the Glu729-Val730 and Glu732-Ala733 bonds are both present in what is predicted to be the surface exposed β3-β4 loop of the Spacer domain, which is in line with their susceptibility to proteolysis (Fig 3). This also suggests that the autolytic reaction may have functional consequences as this Spacer region contains a substrate binding exosite in ADAMTS13 (18-20).

ADAMTS7 cleaves LTBP4

In addition to the autolytic cleavage fragments, TAILS identified forty-five other extracellular matrix proteins that exhibited evidence of increased proteolysis in the presence of active ADAMTS7 (Table S1). To confirm that these findings were a direct consequence of proteolysis by ADAMTS7, we selected candidate substrates for further study. Selection was based on the nature of the scissile bonds, the location of the cleavage within the protein, potential functional consequences of proteolysis and tissue distribution.

Two related proteins, the latent TGF-β binding proteins (LTBP) 3 and 4 were cleaved at Glu-Val and Glu-Ala respectively, matching the most prominent and confirmed autolytic cleavage sites in ADAMTS7 (Glu729-Val730 and Glu732-Ala733). A sequence alignment of the two proteins showed LTBP3 and LTBP4 were both cleaved in the same linker region, between the first EGF-like domain and the hybrid domain (Fig 4A). That the cleavage appeared to occur in a linker region between domains suggested that proteolysis is expected to separate the two cleavage fragments. For LTBP4, this could potentially affect the function of LTBP4 in elastic fibre formation/organisation. Physiologically, LTBP4 contributes to the deposition of tropoelastin on fibrillin-1 microfibrils (21). This occurs by binding of the N-terminal domains of LTBP4 to the fibulin-5/tropoelastin complex and binding of the C-terminal domains of LTBP4 to fibrillin-1 (22). Cleavages by ADAMTS7, therefore, have the potential to separate the fibulin-5/elastin binding region from its fibrillin-1 binding region, thereby disrupting its essential bridging function. Importantly, LTBP4 is also co-expressed with ADAMTS7 in the adult heart and lung (23).

For these reasons, we decided to further investigate the apparent proteolysis of LTBP4 by

ADAMTS7. An N-terminal fragment of LTBP4 (LTBP4S-A) that lacks domains C-terminal of the hybrid domain was expressed in HEK293T cells and the conditioned medium incubated with ADAMTS7-T8, ADAMTS7-Mu or the inactive variant ADAMTS7-Mu (E389Q). Analysis by non-reducing Western blot showed LTBP4S-A cleavage when incubated with ADAMTS7-Mu or ADAMTS7-T8 but not with the inactive control ADAMTS7-Mu (E389Q) (Fig 4B). Coomassie-stained SDS-PAGE analysis of purified LTBP4S-A cleaved by 10 nM purified ADAMTS7-T8 showed multiple cleavage fragments after 8-hour incubation (Fig 4C). These results show that LTBP4 is cleaved by low nM concentrations of ADAMTS7 and is therefore a potential physiological substrate.

The presence of multiple bands following digestion of LTBP4 by ADAMTS7 suggests the presence of additional cleavage sites. Therefore, cleaved and uncleaved LTBP4S-A were labelled with Tandem Mass Tags (TMT) at the N-termini and analysed by LC-MS/MS. TMT labelled peptides (Table S3) revealed a total of twelve scissile bonds, predominantly containing hydrophobic residues Ala, Val and Leu in P1' (Fig 4D), strongly suggesting these are the preferred residues in P1' for ADAMTS7. P1 residues included Glu, but also Arg, Ala, Pro and Gly.

TIMP-4 is an efficient inhibitor of ADAMTS7

Inhibition of ADAMTS7 by endogenous metalloprotease inhibitors (TIMPs) has not been investigated. We therefore investigated if LTPB4S-A cleavage by ADAMTS7 can be specifically inhibited by TIMP members. This revealed that of the four TIMPs, TIMP-4 is the most potent inhibitor of ADAMTS7 (Fig 5A). TIMP-3 showed moderate inhibition and TIMP-1 and TIMP-2 little to no inhibition. To quantify these differences, proteolysis was monitored by densitometry of LTBP4S-A on SDS-PAGE/Coomassie. This showed that in this assay the apparent inhibition constant $K_{i(app)}$ for TIMP-4 was 13 nM, compared to 49 nM for TIMP-3 and >100 nM for TIMP-2 (Fig 5B). These findings confirm that for ADAMTS7, contrary to other ADAMTS family members, TIMP-4 is the most potent inhibitor.

Discussion

Recently, ADAMTS7 has emerged as a modifier of CAD (7,24). However, its substrate specificity is poorly defined and knowledge of cleavage sites is required to understand its physiological role. Here, for the first time, we report scissile bonds targeted by ADAMTS7. These include the autolytic cleavage sites Glu732-Ala733 and Glu729-Val730. We also identified LTBP4 as a novel substrate for ADAMTS7. In LTBP4, the P1' residues were also predominantly Ala and Val, suggesting they are favoured in P1'. Several different LTBP4 residues were found in P1, including Glu, Ala, Arg and Pro. However, mutagenesis of the ADAMTS7 residues Glu729 and Glu730 to Ala reduced autolysis, which shows that ADAMTS7 prefers Glu over Ala at the P1 position. Together, these results shed light on the previously unknown cleavage site specificity of ADAMTS7. This may also benefit the development of small molecule inhibitors, which generally target the so-called specificity pocket (S1') in metalloproteases (25). It has been suggested that small molecule inhibitors of ADAMTS7 could have therapeutic potential in CAD (24,26) given that A*damts7*$^{-/-}$ mice have reduced atherosclerosis in hyperlipidemic mouse models (7). Importantly, the identified cleavage sites in LTBP4 allow the development of neo-epitope antibodies to study whether proteolysis occurs at these sites *in vivo*. Evidence that this may be the case comes from a proteomic analysis of human aorta which identified LTBP4 peptides derived from cleavage events at the sites we identified (E195↓Ala196 and Ala196↓Ala197) (27,28).

We showed that ADAMTS7 cleaves LTBP4 in a way that separates the fibulin-5/elastin binding region from its fibrillin-1 binding region and could, therefore, affect the deposition of Tropoelastin on fibrillin-1 microfibrils (21,29). Whether this occurs in physiological and/or pathological situations needs further investigation. However, ADAMTS7 and LTBP4 have overlapping tissue expression patterns, most notably in cardiac and lung tissue (7,23), suggesting this could be the case. The enzyme concentration at which we detect proteolysis (low nM) also suggests that this could be physiologically relevant. Interestingly, several other ADAMTS and ADAMTS-like proteins have

been implicated in fibrillin-1 microfibril biology, including ADAMTS10, ADAMTS17 and ADAMTS6 (30-33). Phylogenetic analysis of ADAMTS genes shows that ADAMTS7 and 12 are more closely related to ADAMTS17/19/6 and 10 than to the other thirteen ADAMTS family members (34), which may indicate a functional relationship, like that between ADAMTS1, 4 and 5 which are all are all involved in versican and aggrecan turnover.

Autolysis has been reported for several ADAMTS family members (3,35-37). For ADAMTS4 and ADAMTS5, this also involved cleavages in the Spacer domain (35,36). Here, we show that cleavage of the Glu732-Ala733 and Glu729-Val730 in the ADAMTS7 Spacer domain is dependent on ADAMTS7 activity. Our LTBP4 cleavage data further confirmed that ADAMTS7 is capable of cleaving Glu-Ala bonds. These findings strongly suggest that ADAMTS7, like other ADAMTS family members, can cleave itself. Whether this occurs *in vivo* needs further investigation. Autolysis of ADAMTS proteins has so far only been demonstrated in conditioned media and purified ADAMTS proteases. Where conditioned media was used to demonstrate autolysis, the involvement of proteolytic cascades cannot be completely ruled out.

It has previously been shown that ADAMTS activity can be regulated by TIMPs. This has so far only been shown for TIMP-3, which inhibits ADAMTS4 and 5 efficiently (14,38). TIMP-3 inhibits ADAMTS2 very poorly (14) and ADAMTS13 and ADAMTS15 are not inhibited by any of the TIMPs (39). TIMP-4 does not inhibit ADAMTS1, 4 or 5 efficiently (38,40,41). Surprisingly, we showed that TIMP-4 is the most efficient inhibitor of ADAMTS7, although TIMP-3 also showed inhibitory activity. Importantly, TIMP4 inhibited ADAMTS7 efficiently at low nM concentrations, suggesting that this could potentially function as the endogenous inhibitor of ADAMTS7. Both TIMP-4 and ADAMTS7 have a restricted tissue distribution with particularly abundant expression in adult cardiac tissue (42,43), which is therefore a likely site of physiological activity and regulation. Interestingly, *Timp4*$^{-/-}$ mice are more vulnerable to myocardial infarction (44). Our findings suggest unregulated ADAMTS7 may potentially contribute to this phenotype.

Our TAILS analysis identified 45 candidate substrates of ADAMTS7 and in this study we confirmed proteolysis of LTBP4 and autolysis. Whether the other ECM proteins identified are susceptible to proteolysis by ADAMTS7 needs confirmation. One of these, LTBP3, appeared to be cleaved in the same N-terminal linker region as LTBP4. However, the physiological consequence of LTBP3 proteolysis is not immediately clear. The primary function of LTBP3 is reportedly to influence the bioavailability of TGFβ, in cartilage and bone in particular (45). The high MW, latent forms of TGFβ1-3, bind to the middle 8-Cys/TB domain of LTBP3. Mutations in LTBP3 cause dental anomalies and short stature but also appear to increase risk of thoracic aortic aneurysms and dissections (46,47). Binding sites on LTBP3 for fibrillin-1 and/or other ECM molecules have not been identified, suggesting that the effect of proteolysis may be distinct from the effect on LTBP4.

Interestingly, LTBP1 was also identified as a potential ADAMTS7 substrate. LTBP1 exists in two major forms: long (-L)and short (-S), which are transcribed from independent promoters and differ in their N-terminus only (48). The apparent cleavage site, as suggested by our TAILS analysis, is present in the long form (K318-G319), but not in the short form. Although the potential consequence of proteolysis at this site needs characterisation, it is interesting that the long form of LTBP1 (LTBP1L) is primarily important for cardiac and cardiac valve development (49,50).

For COMP, previously reported to be susceptible to proteolysis by ADAMTS7 (15), our TAILS analysis did not identify cleavage products. COMP was expressed by the cells, as the peptide containing the N-terminus of secreted COMP (following removal of the signal peptide) was identified. Using recombinant COMP, we previously found that the ADAMTS7 concentration required for proteolysis of COMP is >500nM (51), which likely exceeds the concentration of ADAMTS7 in our TAILS experiment and is much higher than what is required to cleave LTBP4 (<10nM).

In conclusion, we identified and confirmed a novel substrate of ADAMTS7, LTBP4, the cleavage of which has the potential to impact on elastogenesis, and consequently, elasticity in the cardiovascular system. We shed light on the

previously unknown cleavage site specificity of ADAMTS7 and identified TIMP-4 as an efficient inhibitor, which makes it a likely cardiovascular regulator of ADAMTS7. The autolytic reactions that we report here, may provide an additional mode of regulation. Several other candidate substrates that were identified by TAILS, are of potential interest and require further investigation.

Experimental procedures

Generation of expression vectors

Human ADAMTS7 cDNA was obtained from Source Bioscience (I.M.A.G.E. clone 6650221). The cDNA, including the native signal peptide, was cloned into the pcDNA3.1myc/His expression vector, which adds a myc and 6xHis tag at the C-terminus. Truncated ADAMTS7 variants were truncated after the following amino acids: Pro997 (T4), Gly1414 (Mu), Pro1630 (T8). Point mutants were generated by site directed mutagenesis (KOD Hotstart, Merck). The ADAMTS7-T4 furin cleavage site mutant (FCSM) contains the mutations R68A/R70A/R232A/R236A. The coding sequence of all constructs that were generated was verified by Sanger sequencing (Genewiz UK Ltd). The mammalian expression vector for LTBP4S-A was a generous gift of Tomoyuki Nakamura (Kansai Medical University, Osaka, Japan) and details of its generation have been described previously (21).

iTRAQ-TAILS

The conditioned medium (serum free Dulbecco's Modified Medium) of human skin fibroblasts co-cultured with HEK cells stably expressing ADAMTS7-Mu or inactive ADAMTS7-Mu (E389Q) was prepared for proteomic analysis by LC-MS/MS as previously described (52). Briefly, for each experimental condition, 3.5 x 10^7 HEK cells and 3.3 x 10^7 fibroblasts were co-cultured in serum free Dulbecco's Modified Medium supplemented with amino acids and vitamin C. 120 ml of conditioned medium was harvested per condition and protease inhibitors AEBSF (0.1 mM) and EDTA (1mM) were added. The conditioned medium was concentrated 100x and 500 ug of total protein was denatured with 2.5 M GuHCl, prior to reduction with 1mM tris(2-carboxyethyl)phosphine) at 65°C for 45 mins. Cysteines were alkylated with 5 mM iodoacetamide for 1 hour at room temperature in the dark. Free amines, including those of neo-N-termini generated by ADAMTS7, were labelled with iTRAQ® labels. Proteins recovered from the "active protease condition" and from the "inactive control condition" were labelled with 2.5 mg iTRAQ® 115 or iTRAQ® 117 respectively. After trypsinization with Trypsin Gold (Promega), most peptides not labelled with iTRAQ were removed by coupling to the amine reactive polymer HPG-ALD (Flintbox) and centrifugal filtration (Amicon Ultra 10kDa MWCO). Mass spectrometry was performed with an ESI-Q Exactive mass spectrometer (coupled to 2D-RP/RP NanoAcquity UPLC) at the Proteomic Facility of the University of Liège. For data analysis, the open source Trans-Proteomic Pipeline (TPP) was used. Peptides of potential interest (Appendix, Table S1) were selected based on labelling at the N-terminus with iTRAQ and overrepresentation in the protease condition (>1.5x) vs control condition. Excluded were peptides that mapped to native N-termini or N-termini immediately following signal peptides or furin cleavage sites. Also excluded were peptides that mapped to proteins that are not secreted.

Expression and purification of ADAMTS7 and LTBP4

ADAMTS7, ADAMTS7 variants and LTBP4S-A were transiently expressed in HEK293T cells in OptiMEM (Invitrogen) using PEI MAX 40K (Polysciences, Inc) as a transfection reagent. HEK cells stably expressing ADAMTS7-Mu, ADAMTS7-Mu (E389Q), and ADAMTS7-T8 were generated using G418 (Sigma Aldrich) as a selection reagent. ADAMTS7-T8 was purified using anion exchange chromatography and gel fitration (53). Briefly, 1L conditioned medium was loaded at pH 7.8, followed by washing of the column with 705 mM NaCl, 20 mM Tris (pH 7.8), 10 mM $CaCl_2$ and eluting with 2M NaCl, 20 mM Tris, pH 7.8 10 mM $CaCl_2$. Gel filtration chromatography was employed using a HiPrep Sephacryl S-200 HR column for further purification and exchanging the buffer into 20mM Tris, 150 mM NaCl, 10 mM $CaCl_2$. Protein purity was assessed by SDS-PAGE/Coomassie staining. Eluted fractions were concentrated 5x using Amicon Ultra centrifugal filter units (MWCO 100 kDa) and the purified enzyme was aliquoted and stored at -80 °C until use in proteolytic activity

assays. LTBP4S-A was purified using ANTI-FLAG® M2 Affinity Gel (Sigma Aldrich) using Flag peptide (Sigma Aldrich) for elution.

SDS-PAGE and Western blotting

For SDS-PAGE analysis, Bolt™ 4-12% (ADAMTS7) or 12% (LTBP4S-A) Bis-Tris Plus Gels (Thermo Fisher) were used. Samples were reduced with 5% β-mercaptoethanol where indicated. ADAMTS7 and ADAMTS7 variants were detected with anti-myc Ab (9E10, Santa Cruz biotechnology). LTBP4S-A was recognised with anti-Flag (OctA probe) Ab sc-66355 (Santa Cruz biotechnology). All primary antibodies were used at 0.2µg/ml in phosphate buffered saline (PBS), 5% nonfat dried milk powder and detected with appropriate horseradish peroxidase (HRP) labelled secondary Ab (DAKO). Immobilon Chemiluminescent HRP substrate (Merck Millipore) was detected with a Chemidoc Touch Imaging system (Bio-Rad). For Coomassie staining, gels were stained for 2 hours with Thermo Fisher Imperial protein stain and destained in water overnight at room temperature on an orbital shaker. Treatment of ADAMTS7-T4 CM with recombinant human furin (PeproTech) was performed at a final furin concentration of 50 nM.

N-terminal sequencing of ADAMTS7 autolytic product

ADAMTS7-T4 was expressed at a large scale (0.5 L), purified using a Ni^{2+}-chelating column (HiTRAP, GE Healthcare), and eluted using an Imidazole gradient (20-250mM). Fractions containing ADAMTS7-T4 and its c-terminal autolytic product were identified using dot blot with the anti-Myc Ab (Santa Cruz). Protein purity of these samples was assessed by SDS-PAGE/Silver staining. Samples were dialysed against 20mM Tris, pH 7.5, 150 mM NaCl, 5 mM $CaCl_2$, and concentrated 10x using Amicon Ultra centrifugal filter units, MWCO 10 kDa (Merck). ADAMTS7-T4 and its C-terminal autolytic product were separated by SDS-PAGE using Bolt™ 4-12% Bis-Tris Plus Gels (Thermo Fisher) and transferred to PVDF (Millipore Immobilon PSQ) with Bolt Transfer Buffer (ThermoFisher) and Trans-Blot® Turbo™ Transfer Instrument (Bio-Rad). Protein bands were visualised with Ponceau S staining (Amresco) and the 45 kDa autolytic product band was excised and sent to Alphalyse A/S (Denmark) for N-terminal Sequencing.

Molecular modelling of ADAMTS7

The structure of the N-terminal domains (MP-Spacer) of ADAMTS7 was modelled with the Bioinformatics Toolkit of the Max Planck Institute for Developmental Biology, Tübingen, Germany (54,55). The templates used for modelling were the ADAMTS structures: 3GHM, 2RJQ, 2RJP, 4WK7 and 2V4B. Molecular graphics were produced with an open source version of Pymol precompiled by Christoph Gohlke (University of California, Irvine).

LTBP4S-A cleavage assays

Purified LTBP4S-A (10µM) was incubated at 37° C with or without the indicated concentration of purified ADAMTS7-T8 in 20mM Tris (pH7.5), 150mM NaCl, 10mM $CaCl_2$ for the specified period of time. The indicated concentrations of purified ADAMTS7-T8 used in the assays are the concentration of active protease as determined by active-site titration with TIMP-4. Where TIMPs were used in the assay, recombinant human TIMP1, 2, 3 or 4 (R&D systems) were pre-incubated with ADAMTS7-T8 for 1 hour at 37° C. Proteolysis was stopped by addition of Bolt™ LDS Sample Buffer, 5% β-mercaptoethanol and heating to 95° C. Samples were frozen at -20° C until analysis by SDS-PAGE/Coomassie. To measure TIMP-4 inhibition, proteolysis was quantified by densitometry using ImageJ.

Active site titration of ADAMTS7-T8

TIMP-4 was titrated into the LTBP4SA cleavage assays at concentrations ranging 1.75 nM – 60 nM and relative activity was plotted against TIMP-4 concentration to establish the concentration of active protease in purified ADAMTS7-T8 stock solutions retrospectively (56).

Identification of LTBP4S-A cleavage sites

Purified LTBP4S-A (80 µg) was incubated for 25 h with 70 nM purified ADAMTS7-T8 in 50 mM HEPES (pH 7.5), 5 mM $CaCl_2$ in the presence or absence of broad spectrum metaloprotease inhibitor GM6001 (90 uM). Samples were analysed by SDS-PAGE/Coomassie to confirm proteolysis and the absence thereof in the cleavage and control

condition respectively. New N-termini generated by ADAMTS7 were labelled with Tandem Mass Tags (ThermoFisher) according to the manufacturer's instructions prior to incomplete digest with Trypsin (ThermoFisher), Chymotrypsin (ThermoFisher) and Glu-C (ThermoFisher). LC-MS/MS was performed at the Proteomic Facility of the University of Liège using an Acquity M-Class UPLC (Waters) hyphenated to a Q Exactive (Thermo Scientific), in nanoelectrospray positive ion mode. Data were analysed with Proteome Discoverer version. 2.1.1.21. The protein/peptide identifications were performed against a Bovine background protein database supplemented with the sequence of the human target protein LTBP4. Search parameters were set as "no Enzyme" due to the specific Multi Enzymatic Limited Digestion (MELD) that was applied. Scissile bonds were derived from peptides labelled with TMT at the N-terminus that were identified in the active protease condition, but not in the control condition. All reported peptides have a False Discovery Rate equal or lower than 0.01.

Acknowledgments: We are grateful to Tomoyuki Nakamura (Kansai Medical University, Osaka, Japan) who provided the LTBP4S-A expression vector and to Gabriel Mazzucchelli of the GIGA Proteomics platform, University of Liège, for LC-MS/MS analysis.

Funding: Funding was provided by British Heart Foundation grant PG/18/19/33584 (to R.d.G. and J.T.B.C.), Imperial College (to S.S. and R.d.G.), FRS-FNRS grant 7.6536.18 (to A.C. and C.M), Fonds Léon Frédéricq and ULiège (to A.C.)

Author contributions: A.C. designed experiments, analysed data and wrote the paper. C.M performed experiments, analysed data and wrote the paper. J.T.B.C. designed experiments, analysed data and wrote the paper. S.S. designed experiments, analysed data and wrote the paper. R.d.G. designed and performed experiments, analysed data, prepared the figures and wrote the paper.

Conflict of interest: The authors declare that they have no conflicts of interest with the contents of this article.

References

1. Somerville, R. P., Longpre, J. M., Apel, E. D., Lewis, R. M., Wang, L. W., Sanes, J. R., Leduc, R., and Apte, S. S. (2004) ADAMTS7B, the full-length product of the ADAMTS7 gene, is a chondroitin sulfate proteoglycan containing a mucin domain. *The Journal of biological chemistry* **279**, 35159-35175
2. Gomis-Rüth, F. X. (2009) Catalytic domain architecture of metzincin metalloproteases. *Journal of biological chemistry* **284**, 15353-15357
3. Gendron, C., Kashiwagi, M., Lim, N. H., Enghild, J. J., Thogersen, I. B., Hughes, C., Caterson, B., and Nagase, H. (2007) Proteolytic activities of human ADAMTS-5: comparative studies with ADAMTS-4. *The Journal of biological chemistry* **282**, 18294-18306
4. de Groot, R., Bardhan, A., Ramroop, N., Lane, D. A., and Crawley, J. T. (2009) Essential role of the disintegrin-like domain in ADAMTS13 function. *Blood* **113**, 5609-5616
5. de Groot, R., Lane, D. A., and Crawley, J. T. (2015) The role of the ADAMTS13 cysteine-rich domain in VWF binding and proteolysis. *Blood* **125**, 1968-1975
6. Reilly, M. P., Li, M., He, J., Ferguson, J. F., Stylianou, I. M., Mehta, N. N., Burnett, M. S., Devaney, J. M., Knouff, C. W., Thompson, J. R., Horne, B. D., Stewart, A. F., Assimes, T. L., Wild, P. S., Allayee, H., Nitschke, P. L., Patel, R. S., Myocardial Infarction Genetics, C., et al. (2011) Identification of ADAMTS7 as a novel locus for coronary atherosclerosis and association of ABO with myocardial infarction in the presence of coronary atherosclerosis: two genome-wide association studies. *Lancet* **377**, 383-392
7. Bauer, R. C., Tohyama, J., Cui, J., Cheng, L., Yang, J., Zhang, X., Ou, K., Paschos, G. K., Zheng, X. L., Parmacek, M. S., Rader, D. J., and Reilly, M. P. (2015) Knockout of Adamts7, a novel coronary artery disease locus in humans, reduces atherosclerosis in mice. *Circulation* **131**, 1202-1213
8. Wang, L., Zheng, J., Bai, X., Liu, B., Liu, C. J., Xu, Q., Zhu, Y., Wang, N., Kong, W., and Wang, X. (2009) ADAMTS-7 mediates vascular smooth muscle cell migration and neointima formation in balloon-injured rat arteries. *Circulation research* **104**, 688-698
9. Bengtsson, E., Hultman, K., Duner, P., Asciutto, G., Almgren, P., Orho-Melander, M., Melander, O., Nilsson, J., Hultgardh-Nilsson, A., and Goncalves, I. (2017) ADAMTS-7 is associated with a high-risk plaque phenotype in human atherosclerosis. *Scientific reports* **7**, 3753
10. Kessler, T., Zhang, L., Liu, Z., Yin, X., Huang, Y., Wang, Y., Fu, Y., Mayr, M., Ge, Q., Xu, Q., Zhu, Y., Wang, X., Schmidt, K., de Wit, C., Erdmann, J., Schunkert, H., Aherrahrou, Z., and Kong, W. (2015) ADAMTS-7 inhibits re-endothelialization of injured arteries and promotes vascular remodeling through cleavage of thrombospondin-1. *Circulation* **131**, 1191-1201
11. Mead, T. J., McCulloch, D. R., Ho, J. C., Du, Y., Adams, S. M., Birk, D. E., and Apte, S. S. (2018) The metalloproteinase-proteoglycans ADAMTS7 and ADAMTS12 provide an innate, tendon-specific protective mechanism against heterotopic ossification. *JCI insight* **3**
12. Schunkert, H., Konig, I. R., Kathiresan, S., Reilly, M. P., Assimes, T. L., Holm, H., Preuss, M., Stewart, A. F., Barbalic, M., Gieger, C., Absher, D., Aherrahrou, Z., Allayee, H., Altshuler, D., Anand, S. S., Andersen, K., Anderson, J. L., Ardissino, D., et al. (2011) Large-scale association analysis identifies 13 new susceptibility loci for coronary artery disease. *Nature genetics* **43**, 333-338
13. Pu, X., Xiao, Q., Kiechl, S., Chan, K., Ng, F. L., Gor, S., Poston, R. N., Fang, C., Patel, A., Senver, E. C., Shaw-Hawkins, S., Willeit, J., Liu, C., Zhu, J., Tucker, A. T., Xu, Q., Caulfield, M. J., and Ye, S. (2013) ADAMTS7 cleavage and vascular smooth muscle cell migration is affected by a coronary-artery-disease-associated variant. *American journal of human genetics* **92**, 366-374
14. Brew, K., and Nagase, H. (2010) The tissue inhibitors of metalloproteinases (TIMPs): an ancient family with structural and functional diversity. *Biochimica et biophysica acta* **1803**, 55-71
15. Liu, C. J., Kong, W., Ilalov, K., Yu, S., Xu, K., Prazak, L., Fajardo, M., Sehgal, B., and Di Cesare, P. E. (2006) ADAMTS-7: a metalloproteinase that directly binds to and degrades cartilage oligomeric matrix protein. *FASEB journal : official publication of the Federation of American Societies for Experimental Biology* **20**, 988-990

16. Kleifeld, O., Doucet, A., Auf dem Keller, U., Prudova, A., Schilling, O., Kainthan, R. K., Starr, A. E., Foster, L. J., Kizhakkedathu, J. N., and Overall, C. M. (2010) Isotopic labeling of terminal amines in complex samples identifies protein N-termini and protease cleavage products. *Nature biotechnology* **28**, 281
17. Longpré, J.-M., McCulloch, D. R., Koo, B.-H., Alexander, J. P., Apte, S. S., and Leduc, R. (2009) Characterization of proADAMTS5 processing by proprotein convertases. *The international journal of biochemistry & cell biology* **41**, 1116-1126
18. Pos, W., Crawley, J. T., Fijnheer, R., Voorberg, J., Lane, D. A., and Luken, B. M. (2010) An autoantibody epitope comprising residues R660, Y661, and Y665 in the ADAMTS13 spacer domain identifies a binding site for the A2 domain of VWF. *Blood* **115**, 1640-1649
19. Jin, S. Y., Skipwith, C. G., and Zheng, X. L. (2010) Amino acid residues Arg(659), Arg(660), and Tyr(661) in the spacer domain of ADAMTS13 are critical for cleavage of von Willebrand factor. *Blood* **115**, 2300-2310
20. Akiyama, M., Takeda, S., Kokame, K., Takagi, J., and Miyata, T. (2009) Crystal structures of the noncatalytic domains of ADAMTS13 reveal multiple discontinuous exosites for von Willebrand factor. *Proceedings of the National Academy of Sciences of the United States of America* **106**, 19274-19279
21. Noda, K., Dabovic, B., Takagi, K., Inoue, T., Horiguchi, M., Hirai, M., Fujikawa, Y., Akama, T. O., Kusumoto, K., Zilberberg, L., Sakai, L. Y., Koli, K., Naitoh, M., von Melchner, H., Suzuki, S., Rifkin, D. B., and Nakamura, T. (2013) Latent TGF-beta binding protein 4 promotes elastic fiber assembly by interacting with fibulin-5. *Proceedings of the National Academy of Sciences of the United States of America* **110**, 2852-2857
22. Robertson, I. B., Horiguchi, M., Zilberberg, L., Dabovic, B., Hadjiolova, K., and Rifkin, D. B. (2015) Latent TGF-β-binding proteins. *Matrix Biology* **47**, 44-53
23. Sterner-Kock, A., Thorey, I. S., Koli, K., Wempe, F., Otte, J., Bangsow, T., Kuhlmeier, K., Kirchner, T., Jin, S., and Keski-Oja, J. (2002) Disruption of the gene encoding the latent transforming growth factor-β binding protein 4 (LTBP-4) causes abnormal lung development, cardiomyopathy, and colorectal cancer. *Genes & development* **16**, 2264-2273
24. Arroyo, A. G., and Andres, V. (2015) ADAMTS7 in cardiovascular disease: from bedside to bench and back again? *Circulation* **131**, 1156-1159
25. Fabre, B., Ramos, A., and de Pascual-Teresa, B. (2014) Targeting matrix metalloproteinases: exploring the dynamics of the s1' pocket in the design of selective, small molecule inhibitors. *Journal of medicinal chemistry* **57**, 10205-10219
26. Muller, M., Kessler, T., Schunkert, H., Erdmann, J., and Tennstedt, S. (2016) Classification of ADAMTS binding sites: The first step toward selective ADAMTS7 inhibitors. *Biochemical and biophysical research communications* **471**, 380-385
27. Desiere, F., Deutsch, E. W., King, N. L., Nesvizhskii, A. I., Mallick, P., Eng, J., Chen, S., Eddes, J., Loevenich, S. N., and Aebersold, R. (2006) The PeptideAtlas project. *Nucleic acids research* **34**, D655-D658
28. Doll, S., Dressen, M., Geyer, P. E., Itzhak, D. N., Braun, C., Doppler, S. A., Meier, F., Deutsch, M. A., Lahm, H., Lange, R., Krane, M., and Mann, M. (2017) Region and cell-type resolved quantitative proteomic map of the human heart. *Nature communications* **8**, 1469
29. Robertson, I. B., Horiguchi, M., Zilberberg, L., Dabovic, B., Hadjiolova, K., and Rifkin, D. B. (2015) Latent TGF-beta-binding proteins. *Matrix biology : journal of the International Society for Matrix Biology* **47**, 44-53
30. Hubmacher, D., and Apte, S. S. (2015) ADAMTS proteins as modulators of microfibril formation and function. *Matrix biology : journal of the International Society for Matrix Biology* **47**, 34-43
31. Cain, S. A., Mularczyk, E. J., Singh, M., Massam-Wu, T., and Kielty, C. M. (2016) ADAMTS-10 and-6 differentially regulate cell-cell junctions and focal adhesions. *Scientific reports* **6**, 35956
32. Mularczyk, E. J., Singh, M., Godwin, A. R. F., Galli, F., Humphreys, N., Adamson, A. D., Mironov, A., Cain, S. A., Sengle, G., Boot-Handford, R. P., Cossu, G., Kielty, C. M., and Baldock, C. (2018)

ADAMTS10-mediated tissue disruption in Weill-Marchesani syndrome. *Human molecular genetics* **27**, 3675-3687
33. Wang, L. W., Kutz, W. E., Mead, T. J., Beene, L. C., Singh, S., Jenkins, M. W., Reinhardt, D. P., and Apte, S. S. (2018) Adamts10 inactivation in mice leads to persistence of ocular microfibrils subsequent to reduced fibrillin-2 cleavage. *Matrix biology : journal of the International Society for Matrix Biology*
34. Nicholson, A. C., Malik, S. B., Logsdon, J. M., Jr., and Van Meir, E. G. (2005) Functional evolution of ADAMTS genes: evidence from analyses of phylogeny and gene organization. *BMC evolutionary biology* **5**, 11
35. Georgiadis, K., Crawford, T., Tomkinson, K., Shakey, Q., Stahl, M., Morris, E., Collins-Racie, L., and LaVallie, E. (2002) ADAMTS-5 is autocatalytic at a E753-G754 site in the spacer domain. in *Trans Annu Meet Orthop Res Soc* (pp. 167-167)
36. Flannery, C. R., Zeng, W., Corcoran, C., Collins-Racie, L. A., Chockalingam, P. S., Hebert, T., Mackie, S. A., McDonagh, T., Crawford, T. K., Tomkinson, K. N., LaVallie, E. R., and Morris, E. A. (2002) Autocatalytic cleavage of ADAMTS-4 (Aggrecanase-1) reveals multiple glycosaminoglycan-binding sites. *The Journal of biological chemistry* **277**, 42775-42780
37. Hubmacher, D., Schneider, M., Berardinelli, S. J., Takeuchi, H., Willard, B., Reinhardt, D. P., Haltiwanger, R. S., and Apte, S. S. (2017) Unusual life cycle and impact on microfibril assembly of ADAMTS17, a secreted metalloprotease mutated in genetic eye disease. *Scientific reports* **7**, 41871
38. Kashiwagi, M., Tortorella, M., Nagase, H., and Brew, K. (2001) TIMP-3 Is a Potent Inhibitor of Aggrecanase 1 (ADAM-TS4) and Aggrecanase 2 (ADAM-TS5). *Journal of Biological Chemistry* **276**, 12501-12504
39. Guo, C., Tsigkou, A., and Lee, M. H. (2016) ADAMTS13 and 15 are not regulated by the full length and N-terminal domain forms of TIMP-1,-2,-3 and-4. *Biomedical reports* **4**, 73-78
40. Carlos Rodríguez-Manzaneque, J., Westling, J., Thai, S. N. M., Luque, A., Knauper, V., Murphy, G., Sandy, J. D., and Iruela-Arispe, M. L. (2002) ADAMTS1 cleaves aggrecan at multiple sites and is differentially inhibited by metalloproteinase inhibitors. *Biochemical and biophysical research communications* **293**, 501-508
41. Hashimoto, G., Aoki, T., Nakamura, H., Tanzawa, K., and Okada, Y. (2001) Inhibition of ADAMTS4 (aggrecanase-1) by tissue inhibitors of metalloproteinases (TIMP-1, 2, 3 and 4). *FEBS letters* **494**, 192-195
42. Koskivirta, I., Rahkonen, O., Mayranpaa, M., Pakkanen, S., Husheem, M., Sainio, A., Hakovirta, H., Laine, J., Jokinen, E., Vuorio, E., Kovanen, P., and Jarvelainen, H. (2006) Tissue inhibitor of metalloproteinases 4 (TIMP4) is involved in inflammatory processes of human cardiovascular pathology. *Histochem Cell Biol* **126**, 335-342
43. Rahkonen, O. P., Koskivirta, I. M., Oksjoki, S. M., Jokinen, E., and Vuorio, E. I. (2002) Characterization of the murine Timp4 gene, localization within intron 5 of the synapsin 2 gene and tissue distribution of the mRNA. *Biochimica et biophysica acta* **1577**, 45-52
44. Koskivirta, I., Kassiri, Z., Rahkonen, O., Kiviranta, R., Oudit, G. Y., McKee, T. D., Kyto, V., Saraste, A., Jokinen, E., Liu, P. P., Vuorio, E., and Khokha, R. (2010) Mice with tissue inhibitor of metalloproteinases 4 (Timp4) deletion succumb to induced myocardial infarction but not to cardiac pressure overload. *The Journal of biological chemistry* **285**, 24487-24493
45. Rifkin, D. B., Rifkin, W. J., and Zilberberg, L. (2018) LTBPs in biology and medicine: LTBP diseases. *Matrix Biology* **71-72**, 90-99
46. Huckert, M., Stoetzel, C., Morkmued, S., Laugel-Haushalter, V., Geoffroy, V., Muller, J., Clauss, F., Prasad, M. K., Obry, F., and Raymond, J. L. (2015) Mutations in the latent TGF-beta binding protein 3 (LTBP3) gene cause brachyolmia with amelogenesis imperfecta. *Human molecular genetics* **24**, 3038-3049
47. Guo, D.-c., Regalado, E. S., Pinard, A., Chen, J., Lee, K., Rigelsky, C., Zilberberg, L., Hostetler, E. M., Aldred, M., and Wallace, S. E. (2018) LTBP3 Pathogenic Variants Predispose Individuals to

Thoracic Aortic Aneurysms and Dissections. *The American Journal of Human Genetics* **102**, 706-712

48. Koski, C., Saharinen, J., and Keski-Oja, J. (1999) Independent promoters regulate the expression of two amino terminally distinct forms of latent transforming growth factor-β binding protein-1 (LTBP-1) in a cell type-specific manner. *Journal of Biological Chemistry* **274**, 32619-32630
49. Todorovic, V., Finnegan, E., Freyer, L., Zilberberg, L., Ota, M., and Rifkin, D. B. (2011) Long form of latent TGF-β binding protein 1 (Ltbp1L) regulates cardiac valve development. *Developmental Dynamics* **240**, 176-187
50. Todorovic, V., Frendewey, D., Gutstein, D. E., Chen, Y., Freyer, L., Finnegan, E., Liu, F., Murphy, A., Valenzuela, D., and Yancopoulos, G. (2007) Long form of latent TGF-β binding protein 1 (Ltbp1L) is essential for cardiac outflow tract septation and remodeling. *Development* **134**, 3723-3732
51. Santamaria, S., Crawley, J. T. B., Yamamoto, K., Ahnstrom, J., and de Groot, R. (2017) A comparison of COMP (TSP5) proteolysis by ADAMTS7 and ADAMTS4. *International Journal of Experimental Pathology* **98**, A3-A4
52. Bekhouche, M., Leduc, C., Dupont, L., Janssen, L., Delolme, F., Vadon-Le Goff, S., Smargiasso, N., Baiwir, D., Mazzucchelli, G., Zanella-Cleon, I., Dubail, J., De Pauw, E., Nusgens, B., Hulmes, D. J., Moali, C., and Colige, A. (2016) Determination of the substrate repertoire of ADAMTS2, 3, and 14 significantly broadens their functions and identifies extracellular matrix organization and TGF-beta signaling as primary targets. *FASEB journal : official publication of the Federation of American Societies for Experimental Biology* **30**, 1741-1756
53. de Groot, R. (in press) ADAMTS7: Recombinant protein expression and purification. in *ADAMTS proteins. Methods in Molecular Biology* (Apte, S. S. ed.), Humana Press, New York, NY.
54. Zimmermann, L., Stephens, A., Nam, S. Z., Rau, D., Kubler, J., Lozajic, M., Gabler, F., Soding, J., Lupas, A. N., and Alva, V. (2018) A Completely Reimplemented MPI Bioinformatics Toolkit with a New HHpred Server at its Core. *Journal of molecular biology* **430**, 2237-2243
55. Webb, B., and Sali, A. (2016) Comparative Protein Structure Modeling Using MODELLER. *Current protocols in protein science* **86**, 2.9.1-2.9.37
56. Knight, C. G. (1995) Active-site titration of peptidases. *Methods in enzymology* **248**, 85-101

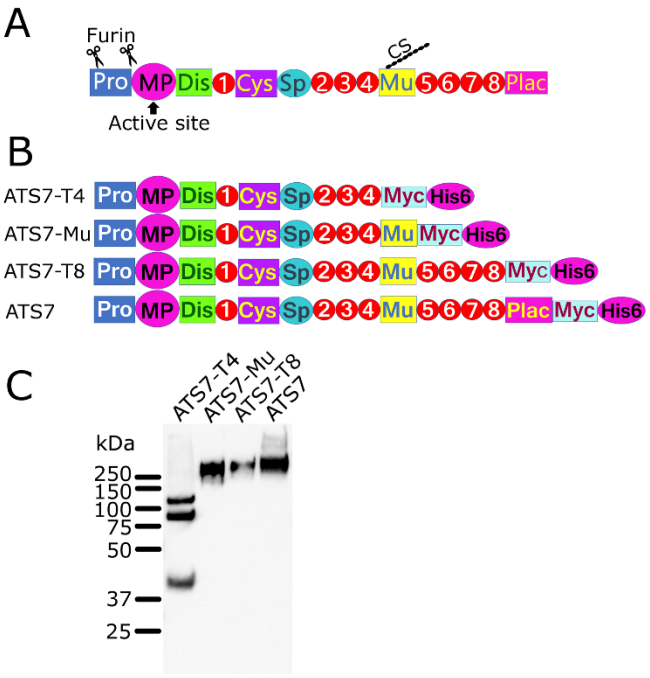

Figure 1. ADAMTS7 constructs. (A) Domain organisation of ADAMTS7. The ADAMTS7 zymogen contains a Prodomain that maintains latency until, upon secretion, furin cleaves at two sites in the Prodomain to generate the mature active form. The metalloprotease domain (MP) contains the active site. The ancillary domains consist of eight thrombospondin type 1 (TSP-1) domains (numbered), a cysteine-rich domain (Cys), Spacer (Sp), mucin-like (Mu) and a protease and lacunin (PLAC) domain. The Mucin-like domain has a chondroitin sulphate (CS) chain attached. (B) Recombinant ADAMTS7 and truncated variants were generated with a C-terminal Myc and His6 tag. (C) Western blot of recombinant ADAMTS7 and truncated variants, detected with an anti-myc tag Ab. The expression of full length ADAMTS7 was very poor and conditioned medium was concentrated ~100x for visualisation on Western blot.

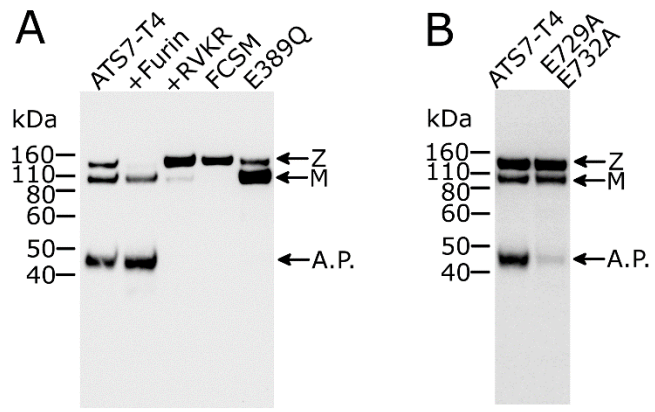

Figure 2. Western blot of ADAMTS7-T4 confirms autolysis as revealed by TAILS. (A) Autolysis can be prevented either by inactivating ADAMTS7 or by abolishing activation by furin. Western blot (reducing) of conditioned medium containing ADAMTS7-T4, detecting with anti myc-tag Ab, shows zymogen (Z), a mature (M) form and a 45 kDA autolytic product (A.P). Conditioned medium was loaded after 2H incubation with either buffer (Lane 1) or 50 nM recombinant furin (Lane 2). Decanoyl-RVKR-CMK is an inhibitor of furin which was added to the medium (10 μM) post transfection to prevent conversion of the latent zymogen to its active (mature) form (Lane 3). Activation was also abolished in the furin cleavage site mutant FCSM (R68A/R70A/R232A/R236A) (Lane 4). The mutation E389Q in the active site of the metalloprotease domain abolishes proteolytic activity and, consequently the appearance of the 45 kDa autolytic product (lane 5). (B) The P1 residues of the autolytic cleavage sites identified by TAILS and N-terminal sequencing were mutated to alanine in ADAMTS7-T4.

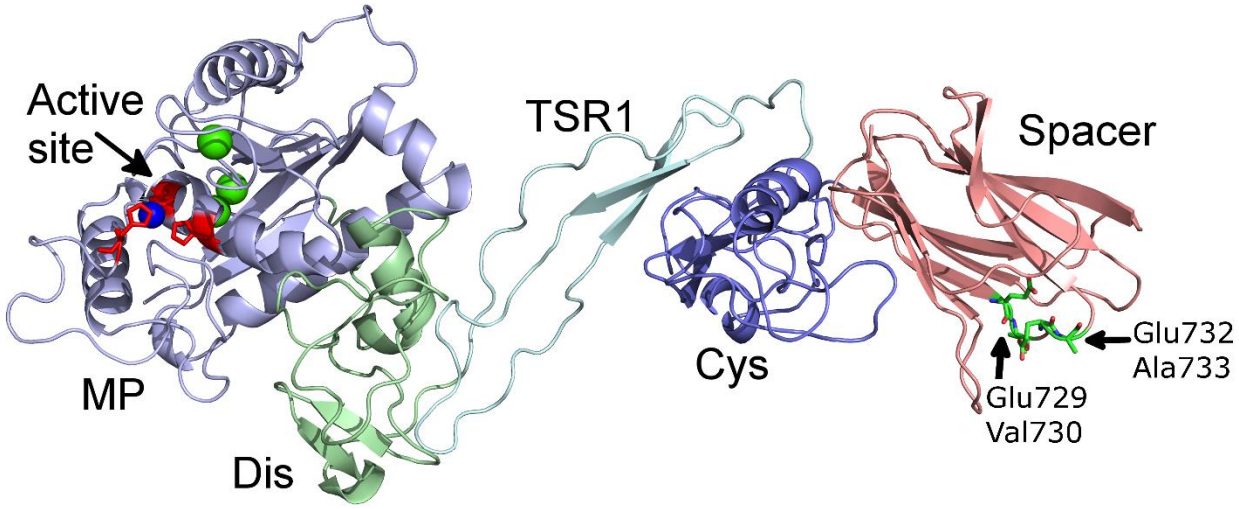

Figure 3. Structural model of ADAMTS7 MP-Spacer domains. The model of the ADAMTS7 Spacer domain structure revealed that the autolytic cleavage sites identified by N-terminal sequencing and TAILS (Glu729-Val730 and Glu732-Ala733) are present in the surface exposed β3-β4 loop of the Spacer domain. The active-site zinc in the MP domain is shown in blue, structural calcium ions are shown in green. The structure of the N-terminal domains of ADAMTS7 (Mp-Spacer) was modelled using the Dis-Spacer structure of ADAMTS13 (3GHM) and ADAMTS1, 4 and 5 MP domain structures (2RJQ, 2RJP, 4WK7, 2V4B).

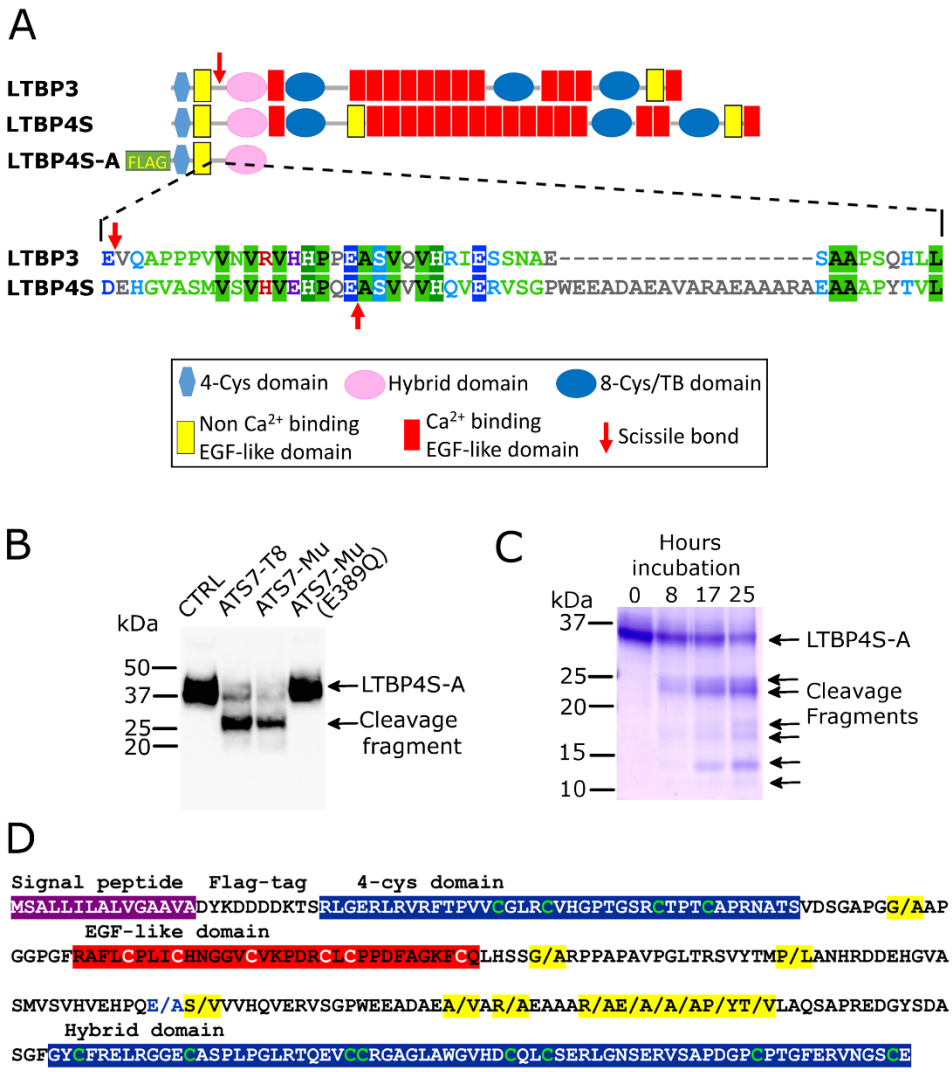

Figure 4. Identification of LTBP4 as a substrate of ADAMTS7. (A) Domain organisation of LTBP3 and LTBP4S, which is the shorter isoform of LTBP4, indicating the location of the scissile bonds (red arrow) that were identified by TAILS. LTBP4S-A is a truncated recombinant variant that contains an N-terminal Flag-tag. For the linker region that contains the identified scissile bonds, an alignment of the amino acid sequence of LTBP3 and LTBP4 is shown, indicating the scissile bonds (red arrows). (B) Western blot of LTBP4S-A conditioned media (anti FLAG Ab) incubated for 17H with buffer (CTRL), purified ADAMTS7-T8 (40nM), ADAMTS7-Mu conditioned medium, or ADAMTS7-Mu (E389Q) conditioned medium. (C). Coomassie stained SDS-PAGE gel of purified LTBP4S-A (10 µm) incubated with 10 nM purified ADAMTS7-T8 for 0, 8, 17 and 25 hours. (D) Amino acid sequence of LTBP4S-A highlighting scissile bonds cleaved by ADAMTS7 (indicated by / and highlighted in yellow) as identified by LC-MS/MS analysis following TMT labelling of cleaved and uncleaved LTBP4S-A.

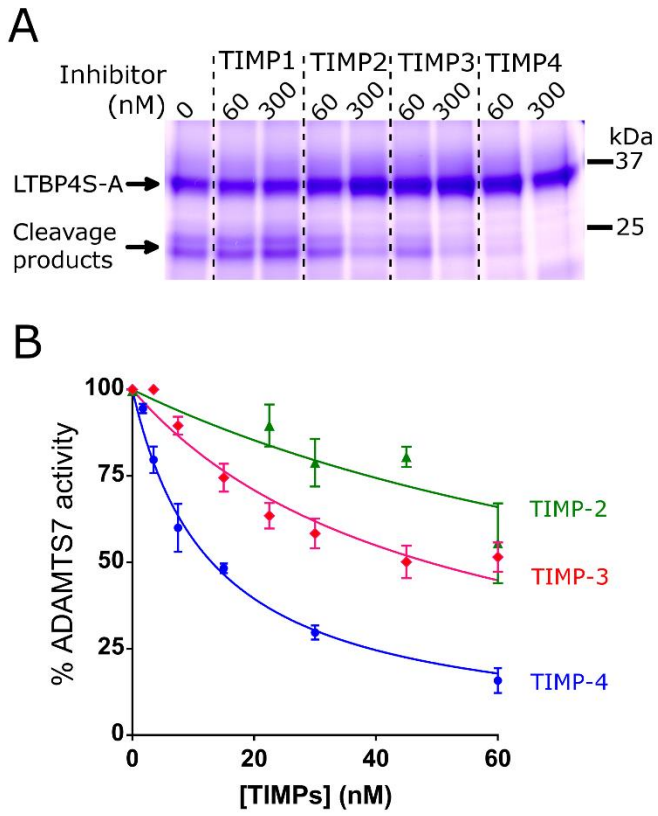

Figure. 5. Inhibition of ADAMTS7 by Tissue Inhibitors of Metalloproteinases (TIMP). (A) ADAMTS7-T8 (9nM) was incubated with LTBP4S-A (20µM) at 37°C for 17 hours in the absence or presence of 60 or 300nM TIMP1,2,3 or 4 and proteolysis was monitored by SDS-PAGE/Coomassie. (B) Various concentrations (1.75-60nM) of TIMP-2 (green triangles), TIMP-3 (pink diamonds) or TIMP-4 (blue circles) were incubated with 18 nM ADAMTS7 and 10µM LTBP4S-A for 17 hours and inhibition of proteolysis was monitored by densitometry of LTBP4S-A on SDS-PAGE/Coomassie. The derived $K_{i(app)}$ for TIMP-4 was 13 nM, compared to 49 nM for TIMP-3 and >100 nM for TIMP-2. Data represent average ±SEM (n=3).

Proteomic discovery of substrates of the cardiovascular protease ADAMTS7

Alain Colige, Christine Monseur, James T.B. Crawley, Salvatore Santamaria and Rens de Groot

J. Biol. Chem. published online March 29, 2019

Supporting Information for:

Proteomic substrate discovery of the cardiovascular protease ADAMTS7

A. Colige[a], C. Monseur[a], J.T.B. Crawley[b], S. Santamaria[b], R. de Groot[b]

[a] Laboratory of Connective Tissue Biology
GIGA, University of Liège
Sart-Tilman
4000 Liège
Belgium

[b] Centre for Haematology
Imperial College London
W12 0NN London
United Kingdom

This PDF file includes:

Table S1: Candidate substrates of ADAMTS7 identified by TAILS

Table S2: ADAMTS7 peptides identified by TAILS suggesting autolysis

Table S3: LTBP4 scissile bonds cleaved by ADAMTS7

Corresponding Author

Dr Rens de Groot
Imperial College London
Centre for Haematology
5th Floor Commonwealth Building
Hammersmith Hospital Campus
Du Cane Road, W12 0NN London
United Kingdom
T: ++44 (0) 20 83 83 22 98
E: R.deGroot@imperial.ac.uk

Table S1. Candidate substrates of ADAMTS7 identified by TAILS

Secreted and transmembrane proteins containing neo-N-termini that were enriched in the presence of active recombinant ADAMTS7 vs inactive ADAMTS7(E389Q). Listed is 1) the ID of the protein in the UniProt database, 2) the full name of the protein, 3) whether the protein is a secreted (S) or a transmembrane (TM) protein, 4) the P1 residue preceding the identified peptide, 5) the amino acid sequence of the identified peptide, 6) the intensity ratio of iTRAQ labels originating from the protease (P) and control (C) condition and 7) the location of the new N-terminus in the structure of the identified protein. ADAMTS7 peptides are listed separately in Table S2.

UniProt ID	Protein name	TM/S	P1	Peptide	P:C	Location new N-terminus
O95450	A disintegrin and metalloproteinase with thrombospondin motifs 2	S	A42	ADPPGGPLGHGAER	1.9	Prodomain
O00468	Agrin	S	K1863	SAGDVDTLAFDGR	1.6	Loop connecting EGF-like 4 and Laminin G-like 3 domains
P22004	Bone morphogenetic protein 6	S	A35	AAAAGGQLLGDGGSPGR	2.4	Propeptide
Q9NYQ6	Cadherin EGF LAG seven-pass G-type receptor 1	TM	R62	ELLDVGR	1.6	Unknown structure
O75976	Carboxypeptidase D	S	G227	EPPALDEVPEVR	3.4	Loop in Peptidase M14 domain
P16870	Carboxypeptidase E	S	R42	LQQEDGISFEYHR	1.7	N-terminus preceding Peptidase M14 domain
P07858	Cathepsin B	S	K79	LPASFDAR	1.7	Loop connecting propeptide with cysteine peptidase domain
P10909	Clusterin	S	R325	ELDESLQVAER	1.8	Clusterin domain
P10909	Clusterin	S	A266	FQHPPTEFIR	1.8	Clusterin domain
P10909	Clusterin	S	P265	AFQHPPTEFIR	1.5	Clusterin domain
P02452	Collagen alpha-1(I) chain	S	A1218	DDANVVR	1.6	Loop preceding C-terminal prodomain. (BMP1 cleavage site)
P02452	Collagen alpha-1(I) chain	S	G174	ISVPGPMGPSGPR	1.5	Non-helical region following the n-terminal propeptide
P02452	Collagen alpha-1(I) chain	S	K781	GESGPSGPAGPTGAR	1.6	Triple-helical region
P02452	Collagen alpha-1(I) chain	S	R1217	ADDANVVR	1.5	Loop preceding C-terminal prodomain
P02461	Collagen alpha-1(III) chain	S	N1251	GQIESLISPDGSR	1.6	C-terminal propeptide (Stalk region)
P20908	Collagen alpha-1(V) chain	S	P435	ANQDTIYEGIGGPR	1.9	Nonhelical region
P39060	Collagen alpha-1(XVIII) chain	S	A1533	DDILASPPR	2.1	NC1 hinge region. Releases endostatin.
P08123	Collagen alpha-2(I) chain	S	P983	SGPVGPAGAVGPR	1.6	Triple helical region
P08572	Collagen alpha-2(IV) chain	S	G1353	FMGNTGPTGAVGDR	1.9	Triple-helical region
P05997	Collagen alpha-2(V) chain	S	G213	SVGPVGPR	2.7	Triple-helical region
P12111	Collagen alpha-3(VI) chain	S	G2240	LIGEQGISGPR	2.2	Collagen-like region
P01034	Cystatin-C	S	R34	LVGGPMDASVEEEGVR	3.2	N-terminal region. Proteolysis may affect inhibitory function.
Q9NT22	EMILIN-3	S	V224	GFGVIPEGLVGPGDR	2.0	Unknown structure
P54756	Ephrin type-A receptor 5	TM	A55	SPSNEVNLLDSR	1.7	Prior to Eph LBD domain
Q8IWU6	Extracellular sulfatase Sulf-1	S	N558	LEEEEELQVLQPR	4.8	PFAM predicted domain DUF3740
Q8IWU6	Extracellular sulfatase Sulf-1	S	Y555	DINLEEEEELQVLQPR	2.4	PFAM predicted domain DUF3740
Q8IWU5	Extracellular sulfatase Sulf-2	S	Y549	HVGLGDAAQPR	2.2	PFAM predicted domain DUF3740
P35556	Fibrillin-2	S	N781	GICENLR	1.6	EGF-like 11 domain
P35556	Fibrillin-2	S	R48	SATAGSEGGFLAPEYR	2.5	Propeptide
P02751	Fibronectin	S	T279	SSGSGPFTDVR	1.7	Loop connecting Fibronectin type-I 5 and Fibronectin type-I 6 domains
P02751	Fibronectin	S	S281	GSGPFTDVR	4.8	Loop connecting Fibronectin type-I 5 and Fibronectin type-I 6 domains
Q86VR8	Four-jointed box protein 1	S	L84	TLAAGADGPPR	1.5	Unknown structure
P22466	Galanin peptides	S	L109	DLPAAASSEDIER	2.7	Galanin message associated peptide (GMAP)
Q08380	Galectin-3-binding protein	S	K441	YSSDYFQAPSDYR	2.2	Unknown structure

Q08380	Galectin-3-binding protein	S	R128	STHTLDLSR	1.8	Loop connecting SRCR and BTB domains
Q08380	Galectin-3-binding protein	S	Y446	FQAPSDYR	2.7	Unknown structure
P28799	Granulins	S	A201	LSSSVMCPDAR	1.5	Loop connecting granulin F and Granulin B
P28799	Granulins	S	S203	SSVMCPDAR	1.5	Loop connecting granulin F and Granulin B
P28799	Granulins	S	S204	SVMCPDAR	1.7	Loop connecting granulin F and Granulin B
P28799	Granulins	S	S205	VMCPDAR	1.7	Loop connecting granulin F and Granulin B
P30443	HLA class I histocompatibility antigen, A-1 alpha chain	TM	V49	GYVDDTQFVR	1.8	Alpha-1 region
P08476	Inhibin beta A chain	S	N98	GYVEIEDDIGR	1.7	Propeptide
P05019	Insulin-like growth factor I	S	A48	GPETLCGAELVDALQFVCGDR	>>1	Loop connecting N-terminal propeptide with IGF I
Q08431	Lactadherin	S	N34	GGLCEEISQEVR	1.6	EGF-like domain
P25391	Laminin subunit alpha-1	S	C873	LGNTDGAHCER	8.1	Laminin EGF-like 8
Q14766	Latent-transforming growth factor beta-binding protein 1	S	K318	GISGEQSTEGSFPLR	2.6	Prior to 4-Cys domain. Present in long form only.
Q9NS15	**Latent-transforming growth factor beta-binding protein 3**	S	E220	VQAPPPVVNVR	1.9	Loop connecting EGF-like domain and hybrid domain
Q8N2S1	**Latent-transforming growth factor beta-binding protein 4**	S	E229	ASVVVHQVER	2.1	Loop connecting EGF-like domain and hybrid domain
Q68D85	Natural cytotoxicity triggering receptor 3 ligand 1	TM	P110	GIQLEEAGEYR	1.8	Ig-like V-type domain
O95502	Neuronal pentraxin receptor	TM	C21	IIASVPLAASPAR	2.2	Loop connecting Signal-anchor with Extracellular region
P14543	Nidogen-1	S	N233	GAYNIFANDR	1.6	NIDO (G1) domain
P07602	Prosaposin	S	N194	GDVCQDCIQMVTDIQTAVR	1.9	Loop connecting propeptide with Saposin B-type 2 domain
O15354	Prosaposin receptor GPR37	TM	R73	EEQGAAFLAGPSWDLPAAPGR	1.8	Extracellular region 1
O75629	Protein CREG1	S	R45	LPPLPPR	1.9	Loop preceding β-barrel
Q92520	Protein FAM3C	S	R41	SALDTAAR	1.6	Known maturation site removing N-terminus
Q04900	Sialomucin core protein 24	TM	T54	TPAPETCEGR	1.7	Extracellular region
O00391	Sulfhydryl oxidase 1	S	R645	DTGAALLAESR	1.5	Unknown structure
Q6ZMP0	Thrombospondin type-1 domain-containing protein 4 (ADAMTSL6)	S	R98	AFADHVVSAVR	2.1	200 amino acid long insert in TSP type-1 1 domain.

Table S2. ADAMTS7 peptides identified by TAILS suggesting autolysis

Neo-N-termini in ADAMTS7 itself that were enriched in the presence of active ADAMTS7 vs inactive ADAMTS7(E389Q) suggest autolysis. Listed are 1) the domain in which the new N-terminus is located 2) the P1 residue preceding the identified peptide sequence 3) the sequence of the identified peptide 4) the intensity ratio of iTRAQ labels originating from the active protease (P) and control (C) condition.

Domain	P1	Peptide	P:C
prodomain	R40	AALDIVHPVR	4.8
prodomain	R76	DAPAFYELQ	>>1
prodomain	R76	DAPAFYEL	4.8
prodomain	R76	DAPAFYELQYR	3.4
prodomain	P79	AFYELQYR	2.6
prodomain	T96	ANQHLLAPGFVSETR	3.2
prodomain	N98	QHLLAPGFVSETR	4.4
prodomain	Q99	HLLAPGFVSETR	7.8
prodomain	L101	LAPGFVSETR	4.0
prodomain	Q194	RGDSSAPSTCGVQVYPELESR	2.5
prodomain	R195	GDSSAPSTCGVQVYPELESR	6.2
prodomain	P201	STCGVQVYPELESR	22.6
prodomain	C204	GVQVYPELESR	4.8
prodomain	C204	GVQVYPELESRR	3.0
prodomain	G205	VQVYPELESR	3.7
prodomain	Q207	VYPELESR	5.8
MP	G328	GDAHPLHHDTAILLTR	2.2
MP	R370	SCSINEDTGLPLAF	3.6
Dis	H504	SKLDAAVDGTR	5.4
Dis	K506	LDAAVDGTR	29.4
cysteine-rich	N637	EYFAEKLR	4.3
cysteine-rich	D646	AVVDGTPCYQVR	3.1
cysteine rich	A647	VVDGTPCYQVR	55.2
cysteine-rich	D650	GTPCYQVR	3.6
cysteine-rich	G673	CDFEIDSGAMEDR	6.0
cysteine-rich	G673	CDFEIDSGAMEDR	3.0

Domain	P1	Peptide	P:C
spacer	E706	AEGLGYVDVGLIPAGAR	3.3
spacer	E708	GLGYVDVGLIPAGAR	4.3
spacer	G709	LGYVDVGLIPAGAR	10.3
spacer	G711	YVDVGLIPAGAR	4.8
spacer	Y712	VDVGLIPAGAR	30.0
spacer	V713	DVGLIPAGAR	3.4
spacer	**E729**	**VAEAANFLALR**	**92.2**
spacer	V730	AEAANFLALR	2.7
spacer	A731	EAANFLALR	3.5
spacer	**E732**	**AANFLALR**	**39.8**
spacer	N758	GDYQVAGTTFTYAR	5.7
spacer	E797	SNPGVHYEYTIHR	2.2
TSP type-1 4	C977	DEAQQPASEVTCSLPLCR	>>1
TSP type-1 4	P983	ASEVTCSLPLCR	18.2
mucin-like	N1194	DFPVGKDSQSQLPPPWR	4.3
mucin-like	K1357	GQPESLSPEVPLSSR	3.7
mucin-like	L1398	AEAGPPADPLVVR	2.2
mucin-like	A1399	EAGPPADPLVVR	4.2

Table S3. LTBP4 scissile bonds cleaved by ADAMTS7. Following LTBP4S-A incubation with ADAMTS7-T8 in the presence (control) or absence of a zinc-chelating small molecule inhibitor, samples were labelled with amine-reactive mass tags (TMT), which labels new N-termini generated by ADAMTS7. After subsequent incomplete digest with Trypsin, Chymotrypsin, and Glu-C, samples were analyzed by LC-MS/MS. Listed are the peptides labelled with TMT at the N-terminus that were found to be abundant in the active protease condition (no inhibitor) but completely absent in the control condition (with inhibitor). The P1 residue preceding the identified peptide is listed with the numbering of LTBP4S (UniProt ID: Q8N2S1-2). Note that using this numbering the P1 residue identified in the original TAILS experiment (Table S1) is E162.

P1	Peptide
G73	AAPGGPGF
G119	ARPPAPAVPGLTR
P138	LANHRDDEHGVAS
P138	LANHRDDEHGVASMVSVHVEHPQEASVVVHQVER
S164	VVVHQVER
A184	VARAEAAARAE
R187	AEAAAR
R187	AEAAARAEAAAP
R193	AEAAAPYT
R193	AEAAAPYTV
E195	AAAPYTVLAQ
E195	AAAPYTVLAQSAPREDG
E195	AAAPYTVLAQSAPREDGYSD
A196	AAPYTV
A196	AAPYTVLAQSAPR
A196	AAPYTVLAQSAPREDG
A197	APYTVLAQSAPR
P199	YTVLAQSAPR
T201	VLAQSAPR